

Preventing oxidative stress: a new role for XBP1

Y Liu^{1,2,3}, M Adachi^{*1,2}, S Zhao³, M Hareyama⁴, AC Koong⁵, Dan Luo⁶, TA Rando⁶, K Imai² and Y Shinomura²

Antioxidant molecules reduce oxidative stress and protect cells from reactive oxygen species (ROS)-mediated cellular damage and probably the development of cancer. We have investigated the contribution of X-box-binding protein (XBP1), a major endoplasmic reticulum stress-linked transcriptional factor, to cellular resistance to oxidative stress. After exposure to hydrogen peroxide (H₂O₂) or a strong ROS inducer parthenolide, loss of mitochondrial membrane potential (MMP) and subsequent cell death occurred more extensively in XBP1-deficient cells than wild-type mouse embryonic fibroblast cells, whereas two other anticancer agents induced death similarly in both cells. In XBP1-deficient cells, H₂O₂ exposure induced more extensive ROS generation and prolonged p38 phosphorylation, and expression of several antioxidant molecules including catalase was lower. Knockdown of XBP1 decreased catalase expression, enhanced ROS generation and MMP loss after H₂O₂ exposure, but extrinsic catalase supply rescued them. Overexpression of XBP1 recovered catalase expression in XBP1-deficient cells and diminished ROS generation after H₂O₂ exposure. Mutation analysis of the catalase promoter region suggests a pivotal role of CCAAT boxes, NF-Y-binding sites, for the XBP1-mediated enhancing effect. Taken together, these results indicate a protective role of XBP1 against oxidative stress, and its positive regulation of catalase expression may at least in part account for this function.

Cell Death and Differentiation (2009) 16, 847–857; doi:10.1038/cdd.2009.14; published online 27 February 2009

High levels of reactive oxygen species (ROS) damage cells and are believed to be associated with various human pathologies, including aging, carcinogenesis and neurodegenerative disorders.^{1–3} To minimize the damage, hosts evolve non-enzymatic and enzymatic antioxidant defenses, the latter include catalase, superoxide dismutases (SODs) and glutathione peroxidases (GPxs). Catalase catalyzes hydrogen peroxide decomposition and has a central role in defense against oxidants generated through various metabolic pathways.⁴ Catalase activity is high in the liver but is also found in the kidney and erythrocytes.⁵ Catalase also plays a crucial role in hematopoietic renewal cells, and maintains bone marrow stem cells.⁶ We recently reported that its expression level in multiple myeloma cells is a pivotal factor determining sensitivity to parthenolide (PTL),⁷ which strongly induces ROS and is a candidate anticancer agent against myeloid leukemia cells.⁸ Catalase gene expression is mainly regulated by CCAAT/enhancer-binding protein- β (C/EBP- β),⁹ which is a member of the basic region/leucine zipper (bZIP) family of transcription factors, and/or by nuclear factor Y (NF-Y), which directly binds to the CCAAT boxes.¹⁰ In addition, SOD1 gene expression is known to be regulated by C/EBP- β , and human phospholipid hydroperoxide GPx is regulated by both C/EBP- ϵ and NF-Y.^{11,12} Thus, the CCAAT-binding proteins¹³ appear to be crucial for the regulation of their basal transcription.

The transcriptional factor X-box-binding protein 1 (XBP1) belongs to the bZIP family and is activated by accumulating

unfolded proteins and other endoplasmic reticulum (ER) stress factors.^{14,15} Upon ER stress, XBP1 mRNA is spliced and creates a translational frame shift.¹⁶ The spliced XBP1 regulates a subset of ER-resident chaperone genes in the unfold protein response and protects cells from ER stress.^{17,18} XBP1 is widely expressed in adult tissues, and essential for hepatogenesis, cardiac myogenesis and plasma cell differentiation.^{19–21} A recent gene profiling study identified many genes as direct targets of XBP1 and their expression is regulated in a distinct cell type- or condition-dependent manner.²² Importantly, the targets include a set of genes linked to DNA damage and repair pathways as well as redox homeostasis and oxidative stress responses. In addition, XBP1 is essential for survival during hypoxia.²³ These accumulating data suggest that XBP1 governs a variety of biological activities.

There are conflicting results regarding XBP1 functions in several types of stress. XBP1 overexpression confers resistance to growth factor deprivation and enhances proliferation independently of growth factors,^{24,25} whereas XBP1 knockdown induces resistance to several ER stresses.^{26,27} Thus, the precise functions of XBP1 remain obscure. As described above, some target genes of XBP1 are classified in categories unrelated to processes associated with ER function. One of the unexpected categories includes genes involved in redox homeostasis and oxidative stress responses,²² which strongly suggests that XBP1 protects cells from oxidative stress, but to our knowledge there are few

¹Division of Molecular Oncology and Molecular Diagnosis, Sapporo Medical University School of Medicine, S-1, W-16, Chuo-Ku, Sapporo 060-8543, Japan; ²First Department of Internal Medicine, Sapporo Medical University School of Medicine, S-1, W-16, Chuo-Ku, Sapporo 060-8543, Japan; ³Department of Neurosurgery, The First Clinical College of Harbin Medical University, Nangang Harbin 150001, PR of China; ⁴Department of Radiation, Sapporo Medical University School of Medicine, S-1, W-16, Chuo-Ku, Sapporo 060-8543, Japan; ⁵Department of Radiation Oncology, Stanford University, Stanford, CA, USA and ⁶Department of Neurology and Neurological Sciences, Stanford University, Stanford, CA, USA

*Corresponding author: M Adachi, First Department of Internal Medicine, Sapporo Medical University School of Medicine, S-1, W-16, Chuo-Ku, Sapporo 060-8543, Japan. Tel: +81 11 611 2111; Fax: +81 11 611 2282; E-mail: adachi@sapmed.ac.jp

Keywords: XBP1; ROS; catalase; oxidative stress; ER stress

Abbreviations: XBP1, X-box-binding protein; ROS, reactive oxygen species; MEF, mouse embryonic fibroblast; ER, endoplasmic reticulum; NF-Y, nuclear factor Y
Received 28.2.08; revised 15.1.09; accepted 19.1.09; Edited by SH Kaufmann; published online 27.2.09

studies of this possibility. In this study, we investigated a possible role of XBP1 in sensitivity to oxidative stress. We found that disruption of XBP1 enhanced sensitivity to oxidative stress, that is, it augmented ROS generation and persistent p38 phosphorylation. Interestingly, we found that XBP1 deletion or knockdown decreased expression of several antioxidant genes, including catalase, SOD1 and TRX1. Our results suggest a novel protective function for XBP1 against oxidative stress, probably, at least in part, through positive regulation of catalase expression.

Results

Loss of XBP1 enhances sensitivity to H₂O₂. To explore a role for XBP1 in cell survival under oxidative stress, we investigated the effects of H₂O₂ on the viability of XBP1 wild-type and XBP1-deficient mouse embryonic fibroblasts (MEFs). At 24 h after H₂O₂ exposure, cell survival was decreased in a dose-dependent manner, and 1 mM H₂O₂ exposure substantially decreased cell viability (approximately 58%) in XBP1-deficient cells, whereas only 12% of the wild-type cells lost their viability (Figure 1a). Pretreatment with the free radical scavenger L-N-acetylcysteine (L-NAC) clearly

decreased H₂O₂-induced cell death in both MEF cells (Figure 1b). The enhanced sensitivity to H₂O₂ was also exhibited by an increased loss of mitochondrial membrane potential (MMP), and this loss was almost completely inhibited by L-NAC (Figure 1c), indicating that under oxidative stress, more extensive mitochondrial damage occurred in XBP1-deficient cells.

Loss of XBP1 specifically enhances sensitivity to oxidative stress.

The sesquiterpene lactone, parthenolide (PTL), the principal active component in feverfew (*Tanacetum parthenium*) used for fever, migraine and arthritis, induces intracellular oxidative stress, which is manifested by elevated ROS levels.^{7,8} Similar to H₂O₂, PTL substantially decreased cell viability in XBP1-deficient cells, but had much less of an effect in XBP1 wild-type cells (Figure 2a), whereas two different types of anticancer agents VP16 (topoisomerase II inhibitor) and FK228 (HDAC inhibitor) induced cell death similarly in both MEF cells. PTL-induced cell death was almost completely blocked by L-NAC (Figure 2b). In XBP1-deficient cells, more extensive loss of MMP occurred, but similar levels of MMP disruption were observed with VP16 or FK228 (Figure 2c). Like H₂O₂,

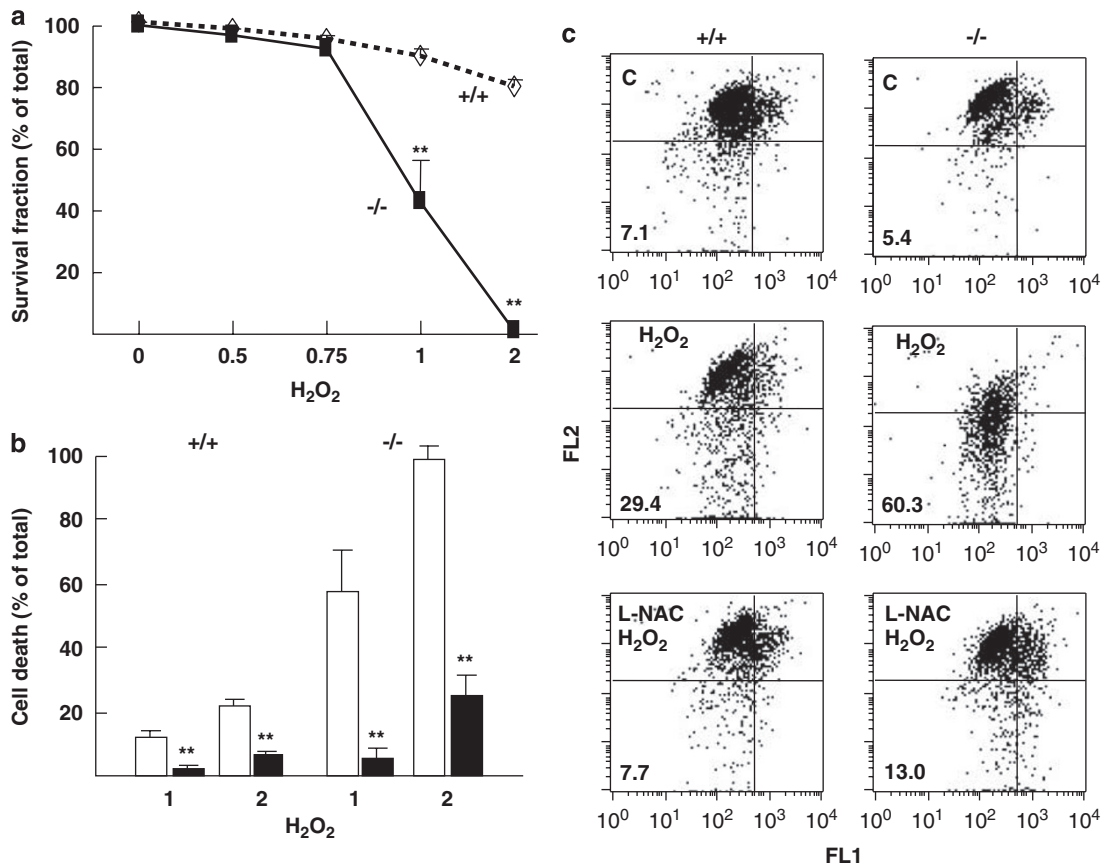


Figure 1 Cell death in H₂O₂-treated MEFs. (a) Trypan blue exclusion assay. Cell survival fraction of XBP1 +/+ (broken line) and -/- (thick line) MEF cells at 24 h after exposure to H₂O₂ at indicated doses (mM). ***P* < 0.01 compared with +/+ cells. (b) Cell death at 24 h after H₂O₂ exposure (mM) with (closed bars) or without (open bars) pretreatment of 5 mM L-NAC for 2 h. In (a, b), error bars indicate the mean ± S.D. of data from three separate experiments. ***P* < 0.01 compared with L-NAC untreated cells. (c) Disruption of Δψ_m. Cells were treated with 1 mM H₂O₂ for 12 h with or without 5 mM L-NAC pretreatment, incubated with DePsipher solution, and intracellular fluorescence was detected. Numbers indicate % of cells showing loss of Δψ_m

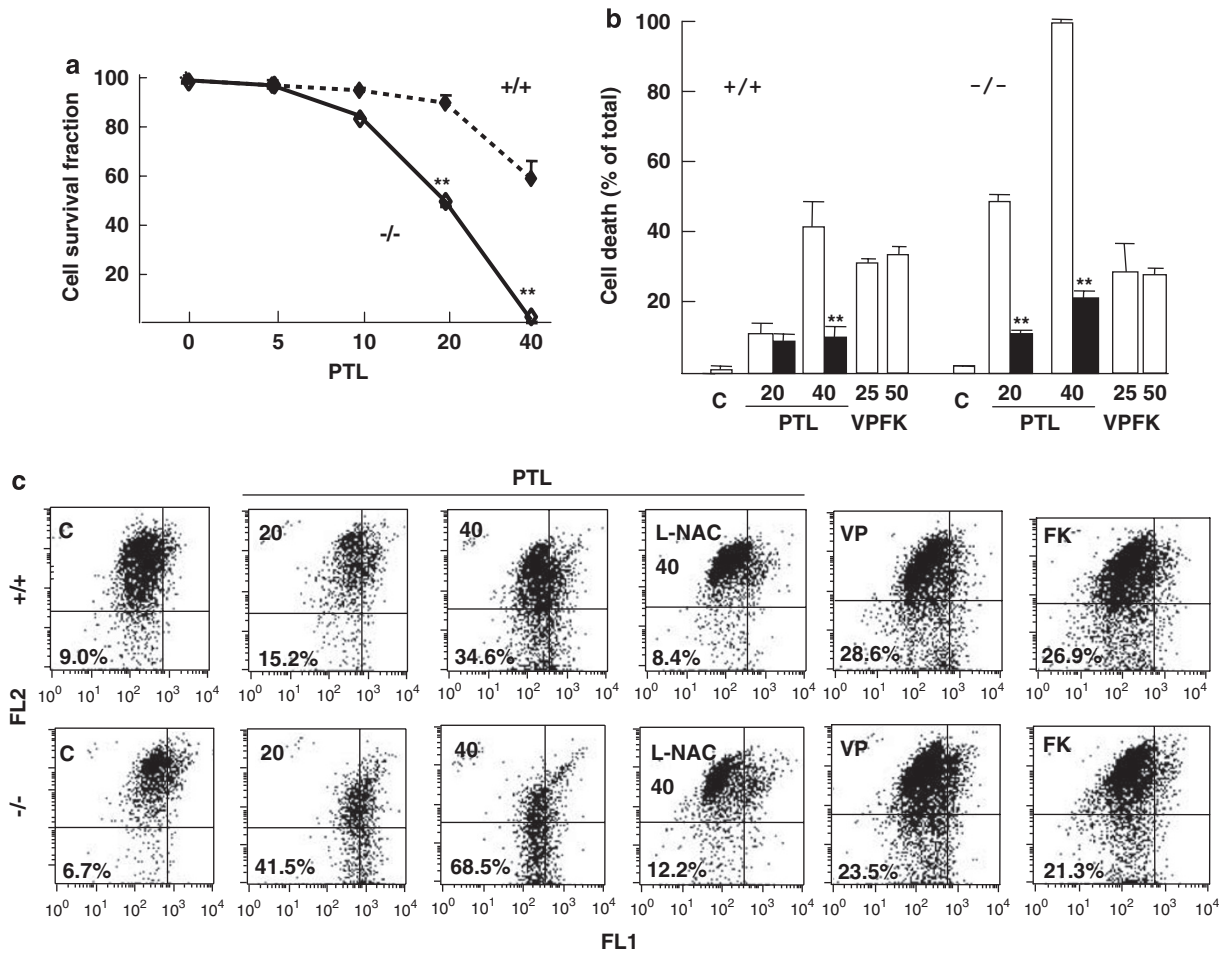


Figure 2 Cell death in PTL-treated MEFs. (a) Trypan blue exclusion assay. Cell survival fraction of XBP1 +/+ (broken line) and -/- (thick line) MEF cells at 24 h after treatment with PTL at indicated doses (μ M). ** $P < 0.01$ compared with +/+ cells. (b) Cell death at 24 h after PTL (μ M), 25 μ g/ml VP16 (VP) or 50 nM FK228 (FK) treatment with (closed bars) or without (open bars) pretreatment of 5 mM L-NAC for 2 h. In (a, b), error bars indicate the mean \pm S.D. of data from three separate experiments. ** $P < 0.01$ compared with L-NAC untreated cells. (c) Disruption of $\Delta\psi/m$. Cells were treated with the indicated agents for 24 h as described in (b), incubated with DePispher solution and intracellular fluorescence was detected. Numbers indicate % of cells showing loss of $\Delta\psi/m$

PTL-induced MMP disruption was also largely blocked by L-NAC (Figure 2c), but L-NAC had little effect on VP16- or FK228-induced MMP disruption (data not shown). These results strongly suggest that disruption of XBP1 specifically enhances sensitivity to oxidative stress.

Enhanced ROS generation in XBP1-deficient cells. To determine the molecular mechanism for the XBP1-mediated protective effect on oxidative stress, we first monitored ROS generation after H_2O_2 exposure in both MEFs. XBP1-deficient cells showed more extensive increases of ROS levels after H_2O_2 treatment (Figure 3a). PTL also induced greater ROS generation in XBP1-deficient MEF cells, an effect which was almost completely canceled by L-NAC pretreatment. Exposure to H_2O_2 or PTL induced prolonged phosphorylation of p38 and/or c-Jun N-terminal kinase JNK in XBP1-deficient cells (Figure 3b). The prolonged phosphorylation of p38 was almost completely inhibited by L-NAC pretreatment (Figure 3c). These data strongly suggest that XBP1 deficiency in MEF cells impairs their antioxidant ability.

XBP1 and antioxidant enzyme expression. To explore the relationship of XBP1 functions with oxidative stress, we compared expression levels of antioxidant enzymes and their related molecules in XBP1 wild-type and -deficient MEFs. Among several antioxidant molecules, we found distinct decreases of catalase, SOD1 and thioredoxin TRX1, but not GPx, mRNA expression in XBP1-deficient cells (Figure 4a). Catalase transcripts were significantly less (approximately three-fold) in XBP1-deficient cells as assessed by real-time PCR. Indeed, catalase protein expression was distinctly low in XBP1-deficient cells (Figure 4b). However, its expression level was not altered by H_2O_2 treatment in both cell types, suggesting that XBP1 may control a steady-state level of catalase. As the difference of expression of catalase was most distinct, we next investigated the role of catalase under H_2O_2 -induced stress in these MEF cells. Exogenous catalase supply strongly inhibited H_2O_2 -induced ROS generation, and its protective effect was almost completely canceled by pretreatment with a catalase inhibitor 3-amino-1,2,4-triazole (AT) (Figure 4c), confirming its specific inhibitory effect on catalase. In XBP1 wild-type MEF,

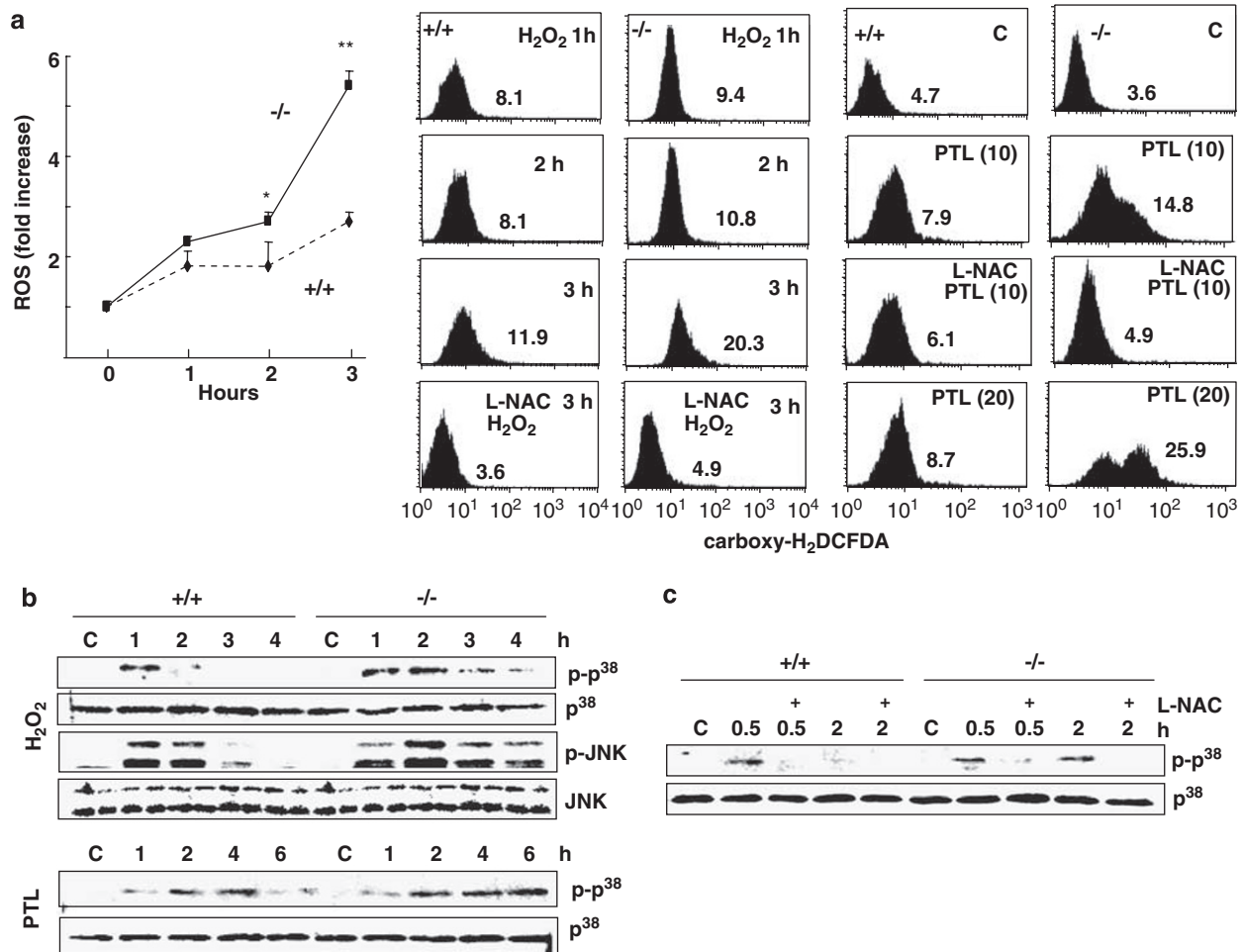


Figure 3 Oxidative stress response. (a) ROS generation. Carboxy-H₂DCFDA fluorescent signals in MEFs after treatment with 1 mM H₂O₂ for 1–3 h or 10–20 μ M PTL for 12 h with or without 5 mM L-NAC pretreatment. In representative histograms, numbers indicate mean fluorescence intensity (MFI) of MEFs. * $P < 0.05$, ** $P < 0.01$ compared with +/+ cells. (b) p38 and JNK phosphorylation. After incubation with 1 mM H₂O₂ or 20 μ M PTL for the indicated hours, p38 and JNK activities were evaluated by western blots using anti-phosphorylated p38 and anti-phosphorylated JNK antibodies, respectively. (c) p38 phosphorylation inhibition by L-NAC. Prior to exposure to 1 mM H₂O₂, MEF cells were pretreated by 5 mM L-NAC (+) for 2 h. Anti-p38 and anti-JNK protein antibodies show equal loading of protein samples

pretreatment with AT strongly enhanced H₂O₂-induced cell death (Figure 4d), nuclear fragmentation (Figure 4e), and induced persistent p38 phosphorylation after H₂O₂ (Figure 4f), exhibiting similar kinetics as observed in the XBP1-deficient MEF.

We next investigated whether spliced XBP1 affected expression levels of these genes. Thapsigargin clearly induced XBP1 splicing and activated its downstream signals, that is, induction of IPK mRNA; however, expressions of catalase, SOD1 and TRX1 mRNA were not increased, but rather decreased (Figure 4g), suggesting that the spliced form of XBP1, XBP1(S) may be unable to positively regulate the expression of these antioxidant genes.

We further investigated the possible linkage of XBP1 to expression of these antioxidant genes *in vivo*. Steady-state level of XBP1 mRNA expression was highest in the murine liver and kidney, and exhibited a similar pattern to the expression of catalase, but SOD1 and TRX1 mRNAs were more broadly expressed (Figure 5a). Indeed, catalase protein expression was highest in the liver, and lowest in the spleen in

both mouse and rat organs (Figure 5b). To confirm their biological activity, we investigated the sensitivity of primary liver and spleen cells to H₂O₂. After H₂O₂ exposure, spleen cells exhibited much more ROS generation (Figure 5c) and cell death (Figure 5d) than hepatic cells, suggesting preferential contribution of XBP1 to catalase expression and cellular antioxidant activity.

XBP1 knockdown decreased catalase expression. To confirm that catalase plays a crucial role for protecting HeLa cells from H₂O₂-induced oxidative stress, we first employed catalase-siRNA SMARTpool transfection. This substantially decreased catalase mRNA expression (Figure 6a) and its products (Figure 6b). The catalase knockdown enhanced cell death (Figure 6b) and loss of MMP after H₂O₂ treatment (data not shown), indicating a crucial function of catalase in HeLa cells to reduce oxidative stress. We next employed transfection of siRNA specifically targeting to XBP1 mRNA. Knockdown of XBP1 strongly decreased XBP1 mRNA expression in HeLa cells and also decreased SOD1 and

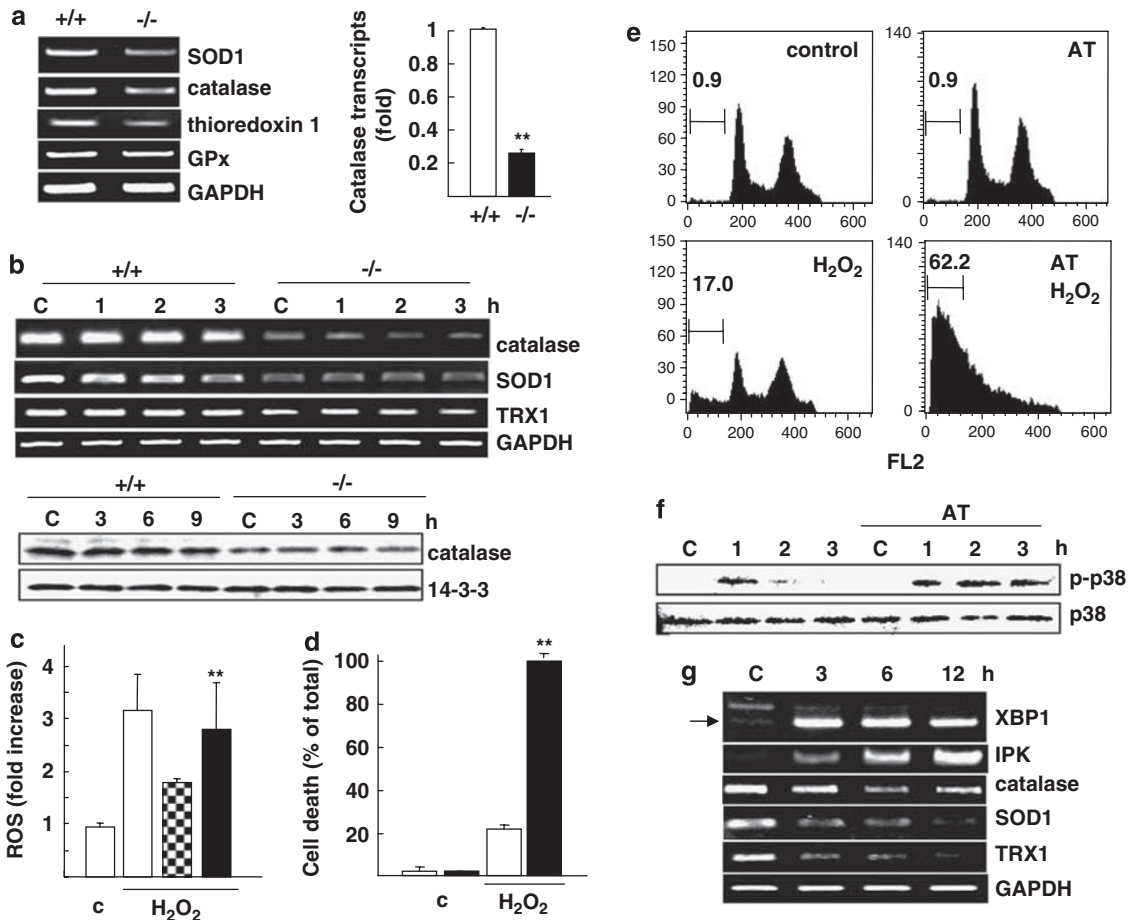


Figure 4 Catalase expression. (a) Total RNAs were harvested from XBP1 $+/+$ and $-/-$ MEF cells and transcripts of the indicated genes were evaluated by RT-PCR. Catalase transcripts were determined by real-time PCR and normalized to GAPDH levels (right panel). $**P < 0.01$ compared with $+/+$ cells. (b) Total RNA (upper panel) and cell lysates (lower panel) were harvested from MEFs after treatment with 1 mM H_2O_2 for the indicated hours. The blot was re-probed with anti-14-3-3 antibody to demonstrate equal loading of protein samples. (c) ROS generation. Carboxy- H_2DCFDA fluorescent signals in MEFs after treatment with 1 mM H_2O_2 for 3 h. XBP1 $+/+$ cells were pretreated with 1 U catalase (mosaic bar), 1 U catalase plus 50 mM AT (closed bar) or without (open bar) for 2 h prior to H_2O_2 exposure. (d) Trypan blue exclusion assay. Cell death of XBP1 $+/+$ MEFs at 24 h after exposure to 1 mM H_2O_2 with (closed bar) or without (open bar) pretreatment with 50 mM AT for 2 h. In (c, d), $**P < 0.01$ compared with AT-untreated cells. (e) Sub-G1 population. XBP1 $+/+$ MEFs were similarly treated as (d) and DNA content in each cell was detected by propidium iodide. Numbers indicate % of sub-G1 population. (f) p38 phosphorylation. After exposure to 1 mM H_2O_2 for 1–3 h with or without 50 mM AT pretreatment for 2 h, p38 activity in XBP1 $+/+$ MEFs was evaluated by western blots using anti-phosphorylated p38 and anti-p38 protein antibodies. (g) Total RNA was prepared from XBP1 $+/+$ MEFs treated with 1 mM thapsigargin for the indicated hours and each transcript was evaluated by RT-PCR. An arrow indicates the spliced form of XBP1. In (a, b, g), GAPDH mRNA levels ensure that the RNAs were correctly quantified. In (a, c, d), error bars indicate the mean \pm S.D. of data from three separate experiments

TRX1 mRNA as observed in XBP1-deficient cells, whereas GPX, OGG1 and NOX2 mRNA expression levels were unchanged (Figure 6a). In contrast, random-siRNA neither decreased catalase, SOD1 nor TRX1 mRNA expression. Nor were expression levels of apoptosis-related molecules Bid, BAX and Bcl-xL altered by XBP1 knockdown. (Figure 6a). Moreover, knockdown of another ER stress mediator PERK did not affect catalase transcripts (Figure 6c), whereas XBP1 knockdown decreased catalase transcripts (approximately two-fold) assessed by real-time PCR (Figure 6d). These data suggest that catalase, probably SOD1 and TRX1, is regulated downstream to an XBP1-mediated pathway. Importantly, XBP1 knockdown actually decreased catalase protein levels, and more strongly elevated ROS generation (Figure 6e) and induced further loss of MMP (Figure 6f) as well as prolonged p38 phosphorylation (Figure 6g) after

0.5 mM H_2O_2 exposure compared with random-siRNA transfectants. Furthermore, extrinsic catalase (0.4 U) supply, which can decrease ROS generation at a similar level of random-siRNA transfectants, but not SOD1, almost completely rescued enhanced H_2O_2 -mediated ROS generation and cell death in XBP1-knockdown cells (Figure 6h). Together with the fact that catalase catalyzes H_2O_2 decomposition and protects cells from oxidative stress, our results strongly suggest that the decreased catalase expression may partly explain why antioxidant activity is reduced in XBP1-deficient cells.

XBP1 overexpression enhanced catalase transcripts. As described above, an unspliced form of XBP1, XBP1(U), may preferentially maintain catalase expression level. To explore the antioxidant activity of different XBP1 forms, XBP1(U),

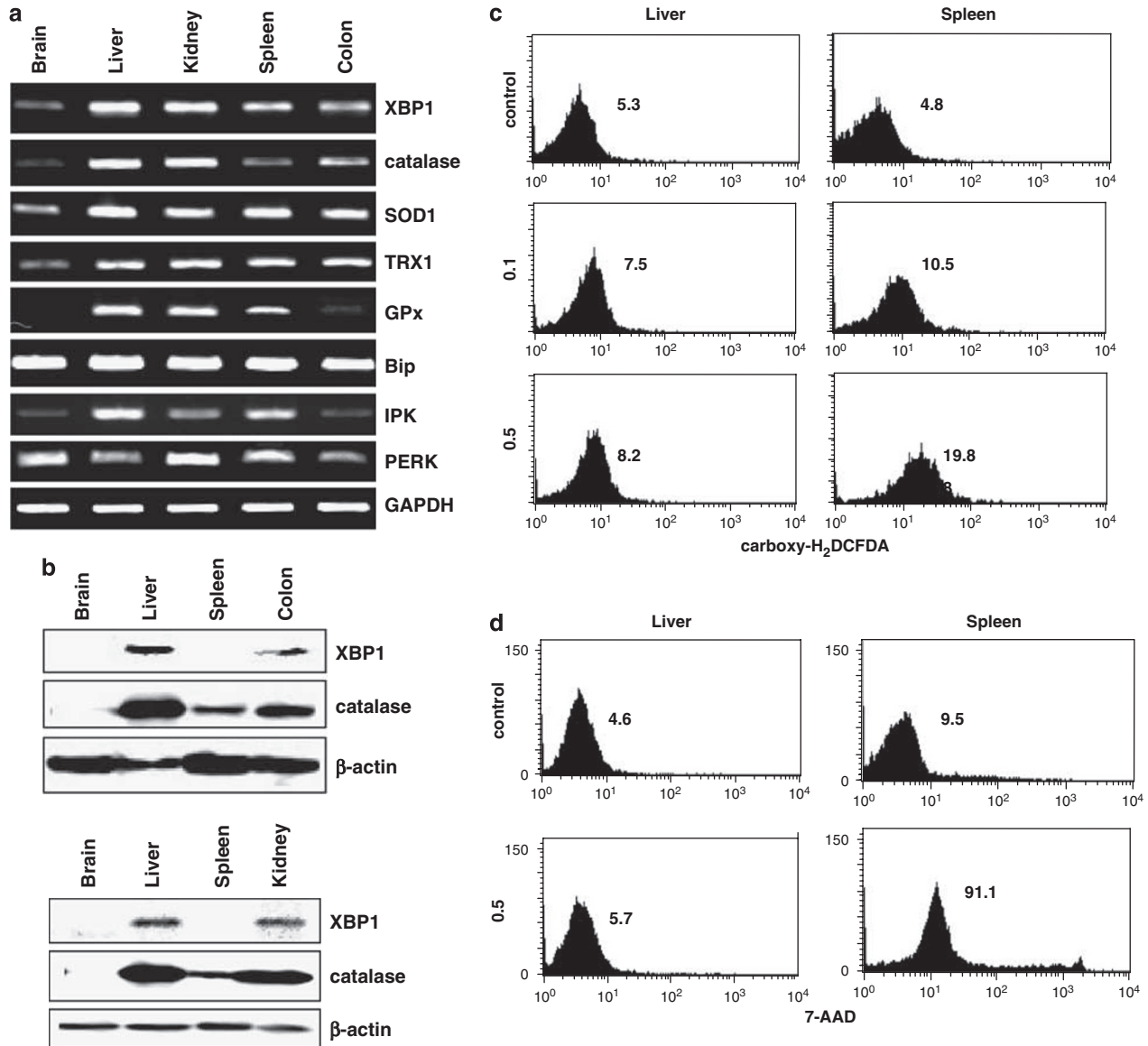


Figure 5 XBP1 expression *in vivo*. (a) Total RNAs were harvested from a SCID mouse and transcripts of the indicated genes were evaluated by RT-PCR. GAPDH mRNA levels ensure that the RNAs were correctly quantified. (b) Western blot analysis of XBP1 and catalase expression in mouse (upper panel) and Wistar rat organs (lower panel). The blot was re-probed with anti- β -actin antibody to demonstrate equal loading of protein samples. (c) ROS generation. Carboxy- H_2 DCFDA fluorescent signals (MFI) in the indicated primary cells after treatment with H_2O_2 (mM) for 1 h. (d) Cell death of primary cells described in (c) assessed by 7-AAD. Cells were harvested at 4 h after exposure to 0.5 mM H_2O_2 , and increased fluorescence indicates cell death. In (c, d), representative histograms are shown and numbers indicate MFI

XBP1(S) and a stable form of XBP1(U), XBP1(KKK), were transiently transfected into XBP1-deficient MEF cells. Although XBP1(S) could not clearly increase catalase expression, XBP1(U) and XBP1(KKK) clearly increased catalase mRNA and its products (Figure 7a), and significantly decreased H_2O_2 -induced ROS generation (Figure 7b).

Next, we investigated the effect of XBP1 overexpression on the promoter activity of catalase 5'-flanking region. The reporter vectors carrying several deletion mutants of the 5'-flanking sequence were transiently transfected into XBP1-deficient MEFs with MOCK or XBP1(U) expression vectors. Although a previous study showed that the pGL3-Enhancer CAT(-191/+68) reporter construct had the highest promoter

activity in the murine myoblast cells,¹⁰ the construct showed the lowest luciferase activity in the XBP1-deficient cells, and XBP1(U) significantly rescued the activity (Figure 7c), demonstrating that XBP1 actually activates catalase gene expression, and suggesting that XBP1-mediated regulatory elements may be located between -191 to +68. The XBP1(U)-mediated enhancing effect was not observed in XBP1 wild-type MEF, and oxidative stress did not affect catalase transcription (Figure 7d), confirming the data shown in Figure 4b.

This region contains no distinct XBP1-binding sites, but has several potential transcriptional factor-binding sites. Previous studies indicate that three CCAAT boxes are considered

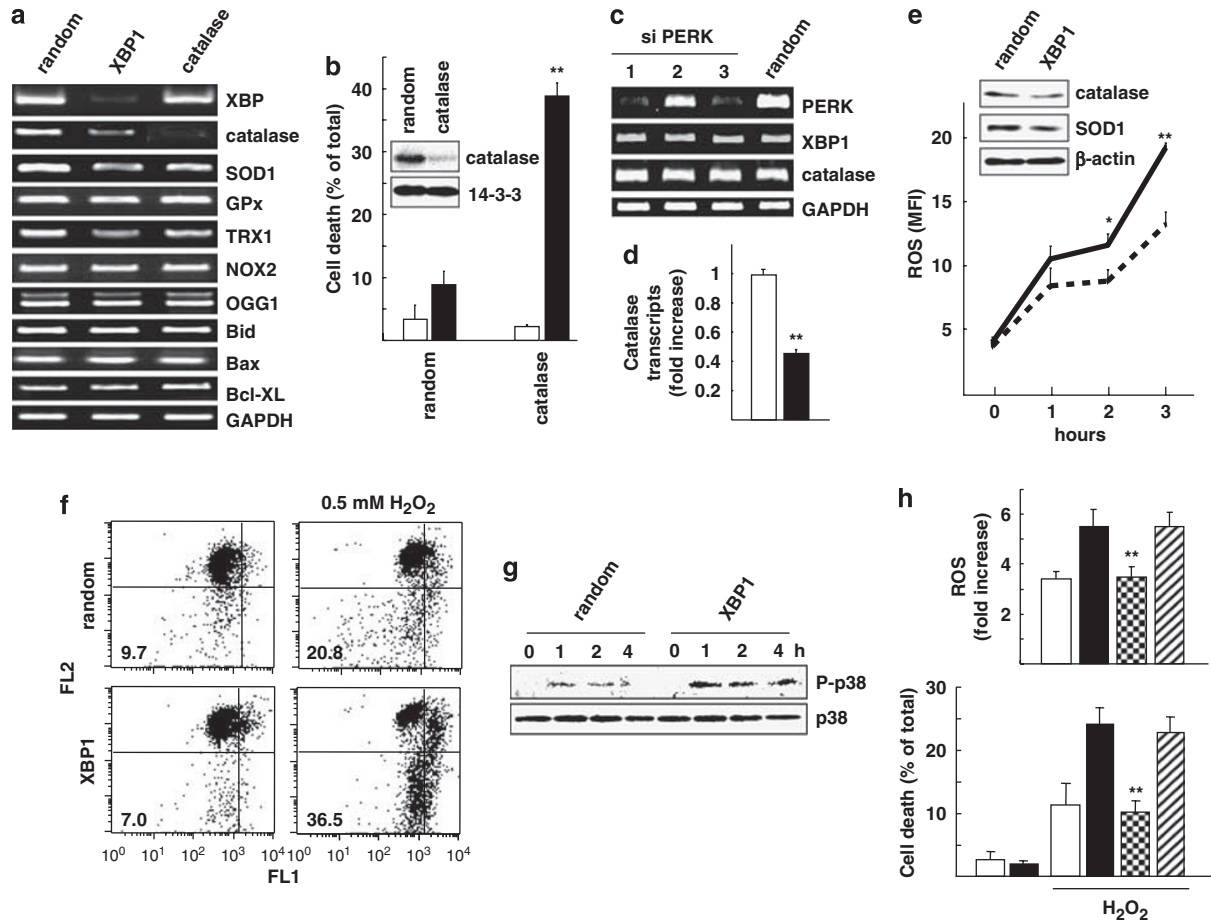


Figure 6 Knockdown of XBP1 transcripts in HeLa cells. (a) RT-PCR. Total RNAs after twice transfection with siRandom (random), siXBP1 (XBP1) or siCatalase (catalase) and the indicated genes were investigated by RT-PCR. (b) Trypan blue exclusion assay. After transfection with siRandom or siCatalase, cells were exposed to 0.5 mM H₂O₂ (closed bars) for 10 h. Catalase knockdown was evaluated by western blot analysis. (c) RT-PCR. Total RNAs were harvested after transfection with siRandom (random) or three different siPERK (PERK) and the indicated genes were analyzed. In (a, c), GAPDH shows that the RNAs were correctly quantified. (d) Quantitative catalase transcripts after XBP1 knockdown. After siRandom (open bar) or siXBP1 (closed bar) transfection, catalase transcripts were determined by real-time PCR and normalized to GAPDH levels. (e) ROS generation. Carboxy-H₂DCFDA fluorescent signals (MFI) in siRandom (broken line) or siXBP1 (thick line) transfectants after treatment with 0.5 mM H₂O₂ for 1–3 h. Expression of the indicated proteins was evaluated by western blot (upper panel). In (b, d, e), **P* < 0.05, ***P* < 0.01 compared with siRandom transfectants. (f) Disruption of $\Delta\psi_m$. Cells were treated with 0.5 mM H₂O₂ for 12 h after four times transfection with siRandom or siXBP1 and MMP was measured. Numbers indicate % of cells showing loss of $\Delta\psi_m$. (g) Prolonged p38 phosphorylation. After transfection as in (f), cells were exposed to 0.5 mM H₂O₂ for indicated hours and p38 phosphorylation was evaluated by western blot analysis. (h) Rescue by catalase supply. Upper panel: ROS generation at 3 h after 0.5 mM H₂O₂ in siRandom (open bar), siXBP1 (closed bar) and siXBP1 transfectants pretreated with 0.4 U catalase (mosaic bar) or 1 U SOD1 (striped bar). In siXBP1 transfectants, 0.4 U catalase decreased ROS generation similar to siRandom transfectants. Lower panel: cell death assessed by Trypan blue exclusion assay at 10 h after 0.5 mM H₂O₂. In (h), ***P* < 0.01 compared with siXBP1 transfectants. In (b, d, e, h), error bars display the mean \pm S.D. of data from three separate experiments

crucial for catalase transcription, and among them, the second CCAAT box plays a pivotal role for NF-Y binding and its promoter activity.^{9,10} In our study, XBP1(U) overexpression clearly enhanced the luciferase activity from pGL3-Basic CAT(–191/+68), but much less from the construct carrying the mutation at the second CCAAT box, and almost completely lost its enhancing effect from that carrying mutations at the second and third CCAAT boxes (Figure 7e). In contrast, mutation at the second GC box exhibited much less effect on the enhancing effect of XBP1(U). These results suggest a requirement of CCAAT box-mediated signals for the effect.

XBP1 and nuclear factors binding to catalase promoter. To explore the mechanism for XBP1-mediated

enhancing effect on catalase transcription, gel shift assays were performed using the catalase promoter probe (–186/–32), which contains all potential transcription factor-binding sites except the third GC box.¹⁰ Nuclear extracts from both MEFs exhibited a similar pattern of multiple shifted bands, but those from XBP1-deficient cells substantially decreased their intensity (Figure 8a). Importantly, the XBP1(U)-rescued cells enhanced the intensity of the largest band, although these nuclear extracts exhibited a similar intensity of shifted bands with the AP2 consensus oligonucleotide probe (Figure 8a and b). Moreover, XBP1(U) overexpression neither affected expression nor intracellular localization of NF-YA, NF-YB and CEBP- β (Figure 8c). Immunoprecipitation assay showed that the catalase promoter DNA-protein complexes actually contain NF-YA, and their interaction appeared to be

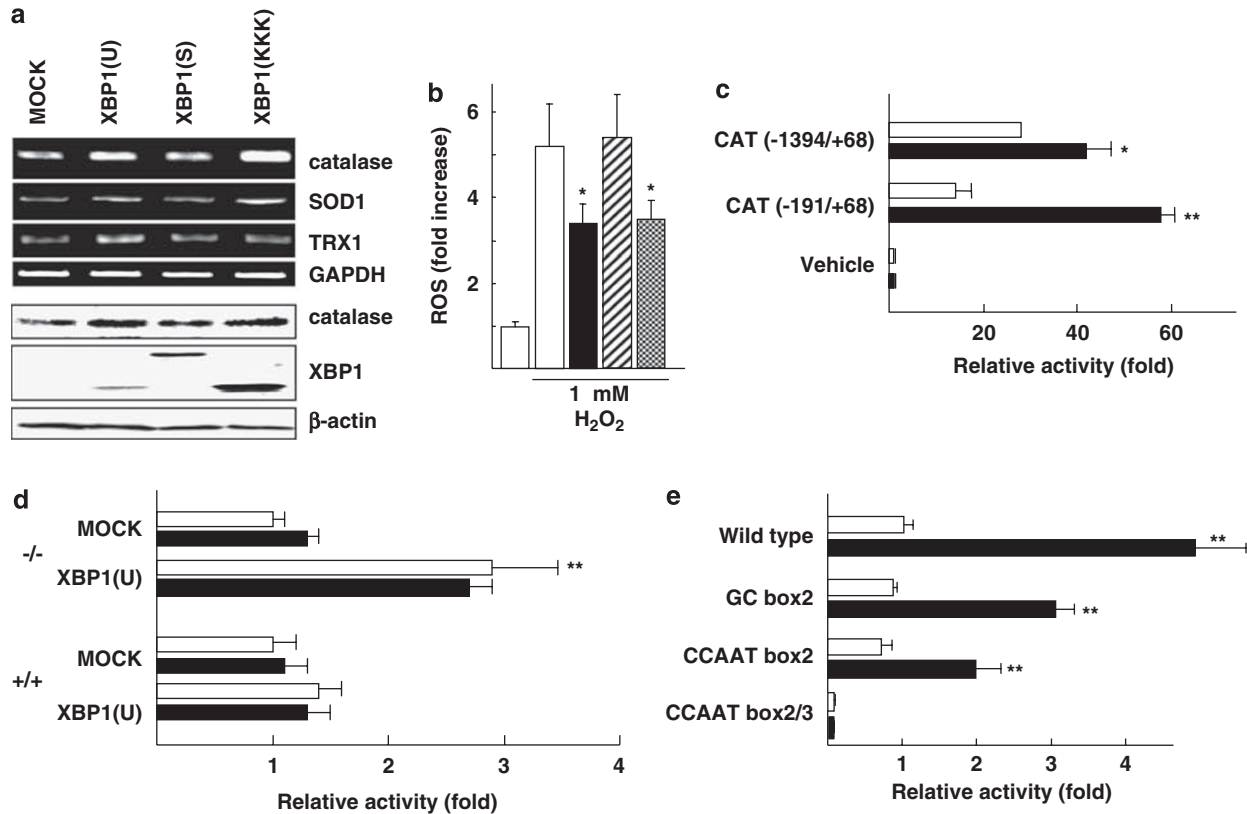


Figure 7 Overexpression of XBP1 and catalase reporter assays. (a) XBP1 overexpression. The indicated forms of XBP1 expression vectors were repeatedly transfected (2–3 times) into XBP1-deficient cells and total RNA (upper panel) and cell lysates (lower panel) were harvested at 7–10 days after first transfection. GAPDH mRNA levels ensure correctly quantified RNAs, whereas β -actin demonstrates equal loading of protein samples. (b) Effect of XBP1 overexpression on ROS generation. In MOCK (open bar), XBP1(U) (closed bar), XBP1(S) (striped bar) and XBP1(KKK) (mosaic bar) transfectants, ROS levels were measured at 3 h after 1 mM H_2O_2 exposure. (c) Effect of XBP1 overexpression on catalase transcription. XBP1-deficient MEFs were transiently co-transfected of the indicated pGL3-Enhancer reporter genes or its vehicle with MOCK (open bar) or XBP1(U) (closed bar). (d) Effect of XBP1(U) on catalase transcription in XBP1 $+/+$ and $-/-$ MEFs. Both MEFs were co-transfected with the pGL3-Enhancer CAT(-191/+68) reporter gene and MOCK or XBP1(U), exposed to 1 mM H_2O_2 (closed bar) for 3 h and harvested. (e) Effect of XBP1 overexpression on pGL3-Basic CAT(-191/+68) reporter genes carrying mutation at the indicated sites. XBP1-deficient cells were transiently co-transfected with the indicated constructs plus XBP1(U) (closed bar) or vehicle (open bar). In (c–e), transcription activity was evaluated 48 h after transfection. Columns display the mean \pm S.D. of data from three separate experiments and * $P < 0.05$, ** $P < 0.01$ compared with MOCK-transfectants

less in XBP1-deficient MEFs and increased by XBP1 overexpression (Figure 8d). In addition, the mutation at the second CCAAT box substantially decreased their DNA-protein complex formation and impaired the enhancing effect of XBP1 overexpression, supporting a crucial role of NF-Y complex for XBP1-mediated catalase transcription.

Discussion

Our results show that XBP1 actually protects cells from oxidative stress. Although several antioxidant genes have been identified as direct targets of XBP1, our experiments are the first to show its functional linkage to oxidative stress. Oxidative stress, H_2O_2 or PTL, induced greater ROS generation and persistent p38 phosphorylation in XBP1-deficient cells implying that loss of XBP1 functions may impair cellular redox homeostasis. To explore how XBP1 functions link to antioxidant activity, we compared expression levels of phase II detoxification enzymes and other antioxidant proteins between XBP1-deficient and wild-type MEFs. We found distinct decreases of antioxidant gene expressions in XBP1-

deficient cells, such as catalase, SOD1 as well as TRX1, but no alteration in GPx, OGG1 and NOX2 expression. As catalase, SOD1 and TRX1 are not direct targets of XBP1, XBP1 probably regulates these genes indirectly.

Among antioxidant genes, catalase appears to be primarily crucial, as its expression is tightly linked to XBP1 expression *in vivo* (Figure 5) and its promoter has CCAAT boxes, targets of NF-Y,¹⁰ which cooperatively functions with XBP1. Namely, XBP1 can activate transcription of target genes carrying the ER stress response element (ERSE) (CCACG) fully when NF-Y binds to the CCAAT part of the ERSE,^{16,22} indicating their tight functional association in ERSE-mediated pathway. Our study showed that mutations at two CCAAT boxes strongly impaired enhancing effects of XBP1 on catalase expression (Figure 7). In addition, gel shift and immunoprecipitation studies showed that in XBP1-deficient cells, XBP1 overexpression enhanced binding of NF-YA to catalase promoter region, but this enhancement was not detected when the catalase promoter carries a mutation at the second CCAAT box (Figure 8). These data suggest that as observed in ERSE-mediated pathway, antioxidant activity of XBP1 may also be

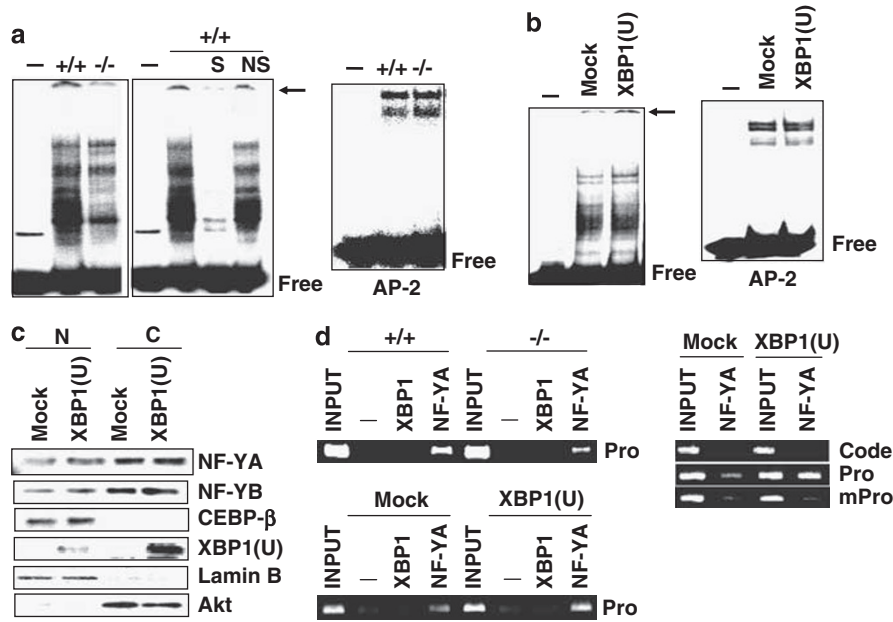


Figure 8 Gel shift and immunoprecipitate assays. (a) The end-labeled catalase promoter probe was incubated with the nuclear extracts from XBP1 +/+ or -/- MEFs and loaded onto non-denaturing gel. The nuclear extract XBP1 (+/+) was preincubated with excess (1 : 100) of the cold probe DNA (S) or unrelated nonspecific DNA (NS). (b) The labeled catalase probe was incubated with the nuclear extracts from XBP1 -/- MEFs transfected with mock or XBP1(U). In (a, b), the same extracts were also incubated with the end-labeled AP2 probe for control study and the arrows indicate shifted bands (the largest complexes). (c) Western blot analysis. Expression of the indicated proteins in the cytoplasmic and nuclear fractions shown in (b) was evaluated by western blots. (d) Immunoprecipitation assays. Unlabeled catalase promoter probe (Pro), its mutant (mPro) or catalase coding region (Code) were incubated with the indicated nuclear extracts and immunoprecipitated with antibodies against XBP1, NF-YA or non-immunized rabbit serum (-). The immunoprecipitates were amplified by corresponding primers. A fixed portion of the total input was also examined by PCR (INPUT)

linked to CCAAT box-mediated signals, probably through NF-Y complexes. As there is no distinct binding site of XBP1 at the catalase promoter region, and no distinct effect of XBP1 on NF-YA and NF-YB expression levels, it remains largely unknown how XBP1 can regulate NF-Y/catalase promoter complex formation. In addition, we cannot exclude a possibility that XBP1 may inhibit some silencers and activate catalase gene independently of CCAAT box-mediated pathway.

In general, XBP1 is activated in response to ER stress. Our data indicate that XBP1 also functions against oxidative stress. Currently, there are many molecules known to be involved in both stress signals, Heme oxygenase (HO-1) is strongly induced by oxidative stress, and also by ER stress,²⁸⁻³⁰ whereas stress kinases, the MAP kinase family members p38 and JNK are simultaneously activated by both types of stress.^{31,32} In addition, the ER stress-inducible transcription factor ATF4 induces a variety of genes for amino-acid import and for protection from oxidative stress.³³ Thus, accumulating evidence strongly suggests that both stress signals are tightly inter-related. Considering that ROS induce lipid peroxidation and lead to membrane damage in the mitochondria, lysosome and ER organelle,³⁴ simultaneous activation of both ER and oxidative stress responses is rational to maintain viability. In this context, our data enlighten XBP1 as a key molecule governing these stress responses.

XBP1 mRNA is spliced under ER stress and spliced XBP1, XBP1(S), is an active transcription factor.¹⁶ We showed that an ER stress inducer thapsigargin failed to activate catalase transcripts but rather decreased them, although XBP1

splicing clearly occurred (Figure 4). This suggests that although XBP1(U) may be sufficient to positively regulate the expression of catalase, XBP1(S) is inactive. Indeed, overexpression of XBP1(U) strongly increased catalase expression, but XBP1(S) failed (Figure 7). Importantly, reporter and gel shift assays suggest that XBP1(U)-mediated enhancing effect on catalase transcription depends upon CCAAT boxes crucial for NF-Y binding (Figures 7 and 8). Considering that NF-Y is necessary for full activation of ERSE,^{16,22} but IRE activation is not essential,³⁵ XBP1 activation is not necessary in this pathway, either. These data strongly suggest a unique function of XBP1(U) independent of XBP1(S), although previous reports suggest an inhibitory function of XBP1(U) on XBP1(S) through rapid degradation.^{36,37} Obviously, we do not fully understand their precise biological activities.

XBP1 is essential for survival under hypoxic conditions, and positively regulates tumor growth.²³⁻²⁵ This knowledge indicates that XBP1 may have multiple functions against a variety of stresses, an important possibility in cancer cell biology. Considering the process of tumor invasion or metastasis, cancer cells should survive under insufficient ATP, oxygen and nutrition. Consequently, XBP1 overexpression may confer metastatic potential on cancer cells. Indeed, breast cancer cells MCF-1 and T47D stably and abundantly express an active form of XBP1 and no longer require estrogen for cell growth.^{24,25} In this context, XBP1 would be a good candidate as a molecular target for the prevention of cancer metastasis. Conversely, increased XBP1 expression may contribute to a reduction of oxidative stress and prevention of aging. Beyond

question, further studies to define XBP1 functions in oxidative stress are essential.

Materials and Methods

Cell culture. A human cervical cancer cell line, HeLa, obtained from the Japanese Cancer Research Resources Bank (Tokyo, Japan), was grown in RPMI1640 (Sigma, St. Louis, MO, USA) supplemented with 10% fetal calf serum (FCS). XBP1 wild-type and knockout MEFs were maintained in DMEM (high glucose; Sigma) with 10% FCS. Animal experiments were performed in accordance with institutional guidance and approved protocols from Institutional Animal Care and Use Committees of Sapporo Medical University. Primary hepatocytes and spleen cells were isolated from Wistar rat by mechanical disruption, cultured overnight in DMEM (Sigma) with 20% FCS and used for the detection of ROS, and cell death was evaluated by 7-aminoactinomycin (7-AAD; BD Bioscience Pharmingen, Mountain View, CA, USA). To evaluate viability, cells were mixed with the same volume of 0.4% Trypan blue solution, and immediately examined to determine whether they excluded the dye under light microscopical observation. Apoptosis was examined using propidium iodide staining for DNA content analysis (sub-G1).

Reagents and antibodies. HDAC inhibitor bicyclic depsipeptide (FK228) was kindly provided by Fujisawa Pharmaceutical Co. (Osaka, Japan). L-NAC, etoposide, PTL, a catalase inhibitor, AT, catalase (2000–5000 U/mg), SOD1, H₂O₂ and anti- β -actin antibody were from Sigma. The anti-p38, anti-phospho-p38 and anti-pan Akt antibodies were purchased from Cell Signaling Technology (Beverly, MA, USA). The anti-14-3-3, anti-JNK, anti-XBP1, anti-Lamin B, anti-CEBP- β , anti-NF- κ B and anti-NF- κ B antibodies were from Santa Cruz Biotechnology Inc. (Santa Cruz, CA, USA). The anti-phospho-JNK antibody was from Promega Corp. (Madison, WI, USA).

ROS detection. Following treatment, cells were incubated with 10 μ M 5-(and-6)-carboxy-2',7'-dichlorodihydrofluorescein diacetate (carboxy-H₂DCFDA) C-400 (Molecular Probes, Eugene, OR, USA) for 30 min, after which they were washed, and further incubated with complete medium for 2–3 h. ROS generation was determined using a FACScan flow cytometry using CellQuest Software™ and fluorescent signals were displayed as histograms.

Detection of mitochondrial membrane potential ($\Delta\psi$ m). Following treatment, cells were incubated with DePsipher solution (Trevigen, Gaithersburg, MD, USA) for 20 min, after which they were washed with PBS, resuspended with reaction buffer, $\Delta\psi$ m was immediately determined using a FACScan flow cytometer (Becton Dickinson, Mountain View, CA, USA). DePsipher is a lipophilic cation, which aggregates upon membrane polarization and forms an orange-red fluorescent compound. MMP disruption blocks aggregation of DePsipher, which reverts to its green monomeric green fluorescent form. Thus, a decrease of the fluorescent signals (FL2) indicates loss of MMP.

Western blotting. After washing with ice-cold PBS, cells were lysed by adding 200 μ l of RIPA buffer (100 mM NaCl, 2 mM EDTA, 1 mM PMSF, 1% NP-40 and 50 mM Tris-HCl (pH 7.2)). Total cell lysates were collected and their protein concentration was evaluated using a protein assay (Bio-Rad, Melville, NY, USA). The lysates (20 μ g per lane) were separated by 10–15% SDS-PAGE gels and then transferred to PVDF membranes (Millipore, Bedford, MA, USA) at 20 V for 50 min. Membranes were soaked in 5% bovine serum albumin (Sigma) overnight. The membranes were incubated with primary antibodies overnight at 4°C, and thereafter incubated with the corresponding peroxidase-linked secondary antibodies (Amersham or MBL) for 1 h at room temperature. Signals were developed by a standard enhanced chemiluminescence method following the manufacturer's protocol (Amersham).

Reverse transcriptase-PCR and transfection. Total RNA of HeLa or MEF cells was extracted with TRIzol (BRL Life and Technologies, MD, USA). The indicated cDNAs were amplified from 2 μ g of total RNA using High Capacity cDNA Reverse Transcription Kit (Applied Biosystems) with random primers. The cDNA products were analyzed on 2% agarose gel and confirmed by nucleotide sequencing. The following primer pairs were used for RT-PCR: catalase: 5'-tcgagtgccaactaccagcgtg-3' and 5'-gtactgtccagaagcctggatg-3'; GPX1: 5'-aagagattcgaattcccaagtacg-3' and 5'-accaggaactctcaaggtccagg-3'; SOD1: 5'-ggatgaa

gagagcagcgtgagac-3' and 5'-gtcttctctctctctctccacc-3'; TRX1: 5'-atgtggaagcagatcgagagcaag-3' and 5'-gtggctcaagcttctct-3'; NOX2: 5'-cagctatgaggtggtgag-3' and 5'-actcagatggagatgctttg-3'; OGG1: 5'-tcagctgtgatgtcac-3' and 5'-tgccccatctagcctcc-3'; Bid: 5'-gcatgtcaacagcgttcta-3' and 5'-ggaacctgcacagtggaat-3'; BAX α : 5'-ggaactgatcagaacctca-3' and 5'-tcagccatctctctcaga-3'; Bcl-xL: 5'-atgtctcagagcaaccggga-3' and 5'-ccatagatgtccacaaatgatc-3'; GAPDH: 5'-cgaccactgtgcaagctca-3' and 5'-aggggtctacatggcaactg-3'. Specificity of amplified PCR fragments were confirmed by DNA sequence analysis.

Quantitative PCR. Quantitative PCR was carried out using an ABI Prism 7000 sequence detection system with standard temperature protocol and QuantiTect SYBR Green PCR Master Mix reagent (Qiagen) in triplicate. Here, 300 nM concentrations of the following primer pairs were used for the reactions: catalase: forward, 5'-tcgagtgccaactaccagcgtg-3'; reverse, 5'-gtactgtccagaagcctggatg-3' and GAPDH: forward, 5'-cgaccactgtgcaagctca-3' and reverse, 5'-aggggtctacatggcaactg-3'. All amplifications were carried out in MicroAmp optical 96-well reaction plates with optical adhesive covers (Applied Biosystems).

Small RNA interference. The 21-nt duplex small interfering (si) RNA pools for catalase (siGENOME SMARTpool M-010021), and control siRNAs (random; 5'-NNACTCTATCTGCACGCTGAC-3') were purchased from Dharmacon (Lafayette, CO, USA). The siRNA for XBP1- or PKR-like ER kinase PERK (Stealth RNAi) was from Invitrogen. Cells (5×10^5 cells per well in a 12-well plate) were incubated for 24 h, and transfected twice or four times with XBP1 siRNA, catalase siRNA, PERK siRNA or control random siRNA (siRandom) duplexes (80 nmol each) using Lipofectamine RNAiMAX (Invitrogen). After 4–7 days, cells were used for the analysis for western blots and cell viability. Transfection efficiency (usually >50%) was assessed in parallel wells by transfection with pEGFP expression vector (BD Biosciences Clontech, Mountain View, CA, USA).

XBP1 overexpression. XBP1-deficient cells were transfected with XBP1 expression vectors,³⁸ that is, an unspliced form of XBP1, XBP1(U), a stable XBP1(U), XBP1(KKK), or a spliced form of XBP1, XBP1(S) using the Lipofectamine LTX Transfection Reagent (Invitrogen). At 7–10 days after repeated transfection (2 or 3 times), cells were harvested for western blots and RT-PCR as well as for the detection of ROS generation.

Catalase reporter assays. As described previously,³⁹ XBP1-deficient cells were transiently transfected with a pRL-TK reporter plasmid (Promega Corp.) and luciferase reporter plasmids containing mouse catalase 5' flanking region,¹⁰ that is, the pGL3-Enhancer (–1394/+68), (–191/+68), pGL3-Basic CAT(–191/+68) and its mutants using the Lipofectamine LTX Transfection Reagent. The mutations are located at the second CCAAT box, the second and third CCAAT boxes, and the second GC box. Catalase transcription was measured as luciferase activity using a luminometer (Mini Lumat LB 9506) 48 h after transfection and normalized to *Renilla* luciferase activity. To detect the effect of XBP1 on catalase transcription, either the XBP1(U) expression vector or its vehicle was co-transfected.

Electrophoretic mobility shift assays. Mobility shift assay was performed using the gel shift assay kit (Promega Corp.). The catalase promoter probe as described below and the AP2 probe (Promega Corp.) were end-labeled with [γ -³²P]ATP (3000 Ci/mmol). The indicated nuclear extracts (5 μ g) were prepared using the CellLytic™ NuCLEAR™ Extraction Kit (Sigma) according to the manufacturer's protocol and incubated with the indicated probe (0.2 pmol) for 20 min at 4°C. The incubated samples were analyzed by 4% non-denaturing polyacrylamide gels.

Immunoprecipitation analysis. The protein–DNA interaction was evaluated using the ChIP assay kit (Upstate Biotechnology) according to the manufacturer's protocol. Nuclear extracts (5 μ g) as described above were incubated with the indicated probe (6 fmol) for 20 min at 4°C and then fixed with formaldehyde for 10 min at 37°C. The DNA–protein complex was immunoprecipitated using anti-XBP1 or anti-NF- κ B (1 μ g) antibody overnight at 4°C and evaluated by PCR amplification using specific primers, that is, primers for catalase promoter, 5'-tctcccagctctctctatc-3' and 5'-tcaggctccacaaatcagcac-3'; for its coding region, 5'-tcgagtgccaactaccagcgtg-3' and 5'-gtactgtccagaagcctggatg-3'. The probes were prepared by PCR amplification using pGL3-Basic CAT(–191/+68), its mutant (mutation at the CCAAT box2) and MEF cDNA as templates. Sensitivity of PCR amplification was evaluated on the recovered probe DNA after incubation with

nuclear extracts and fixation (input fraction). Three independent experiments were performed and similar results were obtained.

Statistical analysis. Statistical analysis was evaluated using Student's *t*-test (SPSS[®] program version 10.1; SPSS, San Rafael, CA, USA). *P* < 0.05 was considered statistically significant.

Acknowledgements. We are grateful to Drs. LH Glimcher and Ann-Hwee Lee (Harvard Medical School) for providing us XBP1^{+/+} and XBP1^{-/-} MEFs, and the XBP1 expression vectors. We also grateful to Dr. Peter M Olley (Sapporo Medical University School of Medicine) for help with preparation of this paper and Ms. Kyoko Fujii (Sapporo Medical University School of Medicine) for technical assistance. This study was supported by the Grants-in-Aid for Scientific Research from the Ministry of Education, Culture, Sports, Science.

- Cooke MS, Evans MD, Dizdaroglu M, Lunec J. Oxidative DNA damage: mechanisms, mutation, and disease. *FASEB J* 2003; **17**: 1195–1214.
- Finkel T, Holbrook NJ. Oxidants, oxidative stress and the biology of ageing. *Nature* 2000; **408**: 239–247.
- Klein JA, Ackerman SL. Oxidative stress, cell cycle, and neurodegeneration. *J Clin Invest* 2003; **111**: 785–793.
- Deisseroth A, Dounce AL. Catalase: Physical and chemical properties, mechanism of catalysis, physiological role. *Physiol Rev* 1970; **50**: 319–375.
- Schisler NJ, Singh SM. Inheritance and expression of tissue-specific catalase activity during development and aging in mice. *Genome* 1987; **29**: 748–760.
- Gupta R, Karpatkin S, Basch RS. Hematopoiesis and stem cell renewal in long-term bone marrow cultures containing catalase. *Blood* 2006; **107**: 1837–1846.
- Wang W, Adachi M, Kawamura R, Sakamoto H, Hayashi T, Ishida T *et al*. Parthenolide-induced apoptosis in multiple myeloma cells involves reactive oxygen species generation and cell sensitivity depends on catalase activity. *Apoptosis* 2006; **11**: 2225–2235.
- Guzman ML, Rossi RM, Karnischky L, Li X, Peterson DR, Howard DS *et al*. The sesquiterpene lactone parthenolide induces apoptosis of human acute myelogenous leukemia stem and progenitor cells. *Blood* 2005; **105**: 4163–4169.
- Taniguchi M, Hashimoto M, Hori N, Sato K. CCAAT/enhancer binding protein- β (C/EBP- β), a pivotal regulator of the TATA-less promoter in the rat catalase gene. *FEBS Lett* 2005; **579**: 5785–5790.
- Luo D, Rando TA. The regulation of catalase gene expression in mouse muscle cells is dependent on the CCAAT-binding factor NF-Y. *Biochem Biophys Res Commun* 2003; **303**: 609–618.
- Seo SJ, Kim HT, Cho G, Rho HM, Jung G. Sp1 and C/EBP-related factor regulate the transcription of human Cu/Zn SOD gene. *Gene* 1996; **178**: 177–185.
- Hattori H, Imai H, Kirai N, Furuhashi K, Sato O, Konishi K *et al*. Identification of a responsible promoter region and a key transcription factor, CCAAT/enhancer-binding protein epsilon, for up-regulation of PHGPx in HL60 cells stimulated with TNF alpha. *Biochem J* 2007; **408**: 277–286.
- Chodosh LA, Baldwin AS, Carthew RW, Sharp PA. Human CCAAT-binding proteins have heterologous subunits. *Cell* 1988; **53**: 11–24.
- Clauss IM, Chu M, Zhao JL, Glimcher LH. The basic domain/leucine zipper protein hXBP-1 preferentially binds to and transactivates CRE-like sequences containing an ACGT core. *Nucleic Acids Res* 1996; **24**: 1855–1864.
- Sriburi R, Jackowski S, Mori K, Brewer JW. XBP1: a link between the unfolded protein response, lipid biosynthesis, and biogenesis of the endoplasmic reticulum. *J Cell Biol* 2004; **167**: 35–41.
- Yoshida H, Matsui T, Yamamoto A, Okada T, Mori K. XBP1 mRNA is induced by ATF6 and spliced by IRE1 in response to ER stress to produce a highly active transcription factor. *Cell* 2001; **107**: 881–891.
- Lee AH, Iwakoshi NN, Glimcher LH. XBP-1 regulates a subset of endoplasmic reticulum resident chaperone genes in the unfolded protein response. *Mol Cell Biol* 2003; **3**: 7448–7459.
- Zhang K, Kaufman RJ. The unfolded protein response: a stress signaling pathway critical for health and disease. *Neurology* 2006; **66**: S102–S109.
- Clauss IM, Gravalles EM, Darling JM, Shapiro F, Glimcher MJ, Glimcher LH. *In situ* hybridization studies suggest a role for the basic region-leucine zipper protein hXBP-1 in exocrine gland and skeletal development during mouse embryogenesis. *Dev Dyn* 1993; **197**: 146–156.
- Reimold AM, Etkin A, Clauss I, Perkins A, Friend DS, Zhang J *et al*. An essential role in liver development for transcription factor XBP-1. *Genes Dev* 2000; **14**: 152–157.
- Reimold AM, Iwakoshi NN, Manis J, Vallabhajosyula P, Szomolanyi-Tsuda E, Gravalles EM *et al*. Plasma cell differentiation requires the transcription factor XBP-1. *Nature* 2001; **412**: 300–307.
- Acosta-Alvear D, Zhou Y, Blais A, Tsikitis M, Lents NH, Arias C *et al*. XBP1 controls diverse cell type- and condition-specific transcriptional regulatory networks. *Mol Cell* 2007; **27**: 53–66.
- Romero-Ramirez L, Cao H, Nelson D, Hammond E, Lee AH, Yoshida H *et al*. XBP1 is essential for survival under hypoxic conditions and is required for tumor growth. *Cancer Res* 2004; **64**: 5943–5947.
- Fujimoto T, Onda M, Nagai H, Nagahata T, Ogawa K, Emi M. Upregulation and overexpression of human X-box binding protein 1 (hXBP-1) gene in primary breast cancers. *Breast Cancer* 2003; **10**: 301–306.
- Gomez BP, Riggins RB, Shajahan AN, Klimach U, Wang A, Crawford AC *et al*. Human X-box binding protein-1 confers both estrogen independence and antiestrogen resistance in breast cancer cell lines. *FASEB J* 2007; **21**: 4013–4027.
- Yokouchi M, Hiramatsu N, Hayakawa K, Okamura M, Du S, Kasai A *et al*. Involvement of selective reactive oxygen species upstream of proapoptotic branches of unfolded protein response. *J Biol Chem* 2008; **283**: 4252–4260.
- Endo S, Hiramatsu N, Hayakawa K, Okamura M, Kasai A, Tagawa Y *et al*. Geranylgeranylacetone, an inducer of the 70-kDa heat shock protein (HSP70), elicits unfolded protein response and coordinates cellular fate independently of HSP70. *Mol Pharmacol* 2007; **72**: 1337–1348.
- Sun J, Brand M, Zenke Y, Tashiro S, Groudine M, Igarashi K. Heme regulates the dynamic exchange of Bach1 and NF-E2-related factors in the Maf transcription factor network. *Proc Natl Acad Sci USA* 2004; **101**: 1461–1466.
- Liu XM, Peyton KJ, Ensenat D, Wang H, Schafer AI, Alam J *et al*. Endoplasmic reticulum stress stimulates heme oxygenase-1 gene expression in vascular smooth muscle. Role in cell survival. *J Biol Chem* 2005; **280**: 872–877.
- Cullinan SB, Zhang D, Hannink M, Arvais E, Kaufman RJ, Diehl JA. Nrf2 is a direct PERK substrate and effector of PERK-dependent cell survival. *Mol Cell Biol* 2003; **23**: 7198–7209.
- Matsuzawa A, Nishitoh H, Tobiume K, Takeda K, Ichijo H. Physiological roles of ASK1-mediated signal transduction in oxidative stress- and endoplasmic reticulum stress-induced apoptosis: advanced findings from ASK1 knockout mice. *Antioxid Redox Signal* 2002; **4**: 415–425.
- Matsukawa J, Matsuzawa A, Takeda K, Ichijo H. The ASK1-MAP kinase cascades in mammalian stress response. *J Biochem* 2004; **136**: 261–265.
- Harding HP, Zhang Y, Zeng H, Novoa I, Lu PD, Calfon M *et al*. An integrated stress response regulates amino acid metabolism and resistance to oxidative stress. *Mol Cell* 2003; **11**: 619–633.
- Ott M, Gogvadze V, Orrenius S, Zhivotovskiy B. Mitochondria, oxidative stress and cell death. *Apoptosis* 2007; **12**: 913–922.
- Yamamoto K, Yoshida H, Kokame K, Kaufman RJ, Mori K. Differential contributions of ATF6 and XBP1 to the activation of endoplasmic reticulum stress-responsive cis-acting elements ERSE, UPR and ERSE-II. *J Biochem* 2004; **136**: 343–350.
- Yoshida H, Oku M, Suzuki M, Mori K. pXBP1(U) encoded in XBP1 pre-mRNA negatively regulates unfolded protein response activator pXBP1(S) in mammalian ER stress response. *J Cell Biol* 2006; **172**: 565–575.
- Tirosh B, Iwakoshi NN, Glimcher LH, Ploegh HL. Rapid turnover of unspliced Xbp-1 as a factor that modulates the unfolded protein response. *J Biol Chem* 2006; **281**: 5852–5860.
- Lee AH, Iwakoshi NN, Anderson KC, Glimcher LH. Proteasome inhibitors disrupt the unfolded protein response in myeloma cells. *Proc Natl Acad Sci USA* 2003; **100**: 9946–9951.
- Zhang Y, Adachi M, Kawamura R, Imai K. Bmf is a possible mediator in histone deacetylase inhibitors FK228 and CBHA-induced apoptosis. *Cell Death Differ* 2006; **13**: 129–140.